

Data-dependent compression of random features for large-scale kernel approximation

Raj Agrawal

CSAIL

Massachusetts Institute of Technology
r.agrawal@csail.mit.edu

Trevor Campbell

Department of Statistics
University of British Columbia
trevor@stat.ubc.ca

Jonathan H. Huggins

Department of Biostatistics
Harvard University
jhuggins@mit.edu

Tamara Broderick

CSAIL
Massachusetts Institute of Technology
tbroderick@csail.mit.edu

Abstract

Kernel methods offer the flexibility to learn complex relationships in modern, large data sets while enjoying strong theoretical guarantees on quality. Unfortunately, these methods typically require cubic running time in the data set size, a prohibitive cost in the large-data setting. Random feature maps (RFMs) and the Nyström method both consider low-rank approximations to the kernel matrix as a potential solution. But, in order to achieve desirable theoretical guarantees, the former may require a prohibitively large number of features J_+ , and the latter may be prohibitively expensive for high-dimensional problems. We propose to combine the simplicity and generality of RFMs with a data-dependent feature selection scheme to achieve desirable theoretical approximation properties of Nyström with just $O(\log J_+)$ features. Our key insight is to begin with a large set of random features, then reduce them to a small number of weighted features in a data-dependent, computationally efficient way, while preserving the statistical guarantees of using the original large set of features. We demonstrate the efficacy of our method with theory and experiments—including on a data set with over 50 million observations. In particular, we show that our method achieves small kernel matrix approximation error and better test set accuracy with provably fewer random features than state-of-the-art methods.

1 Introduction

Kernel methods are essential to the machine learning and statistics toolkit because of their modeling flexibility, ease-of-use, and widespread applicability to problems including regression, classification, clustering, dimensionality reduction, and one and two-sample testing [10, 16, 19, 40]. In addition to good empirical performance, kernel-based methods come equipped with strong statistical and learning-theoretic guarantees [3, 4, 30, 44, 48, 49]. Because kernel methods are nonparametric, they are particularly attractive for large-scale problems, where they make it possible to learn complex, highly non-linear structure from data. Unfortunately, their time and memory costs scale poorly with data size. Given N observations, storing the kernel matrix K requires $O(N^2)$ space. Using K for learning typically requires $O(N^3)$ time, as this often entails inverting K or computing its singular value decomposition.

To overcome poor scaling in N , researchers have devised various approximations to exact kernel methods. A widely-applicable and commonly used tactic is to replace K with a rank- J approximation, which reduces storage requirements to $O(NJ)$ and computational complexity of inversion or singular

value decomposition to $O(NJ^2)$ [17]. Thus, if J can be chosen to be constant or slowly increasing in N , only (near-)linear time and space is required in the dataset size. Two popular approaches to constructing low-rank approximations are random feature maps (RFMs) [12, 25, 32, 38]—particularly random Fourier features (RFFs) [33]—and Nyström-type approximations [13]. The Nyström method is based on using J randomly sampled columns from K , and thus is data-dependent. The data-dependent nature of Nyström methods can provide statistical guarantees even when $J \ll N$, but these results either apply only to kernel ridge regression [14, 36, 52] or require burdensome recursive sampling schemes [28, 31]. Random features, on the other hand, are simple to implement and use J random features that are data-independent. For problems with both large N and number of covariates p , an extension of random features called *Fast Food RFM* has been successfully applied at a fraction of the computational time required by Nyström-type approximations, which are *exponentially* more costly in terms of p [26]. The price for this simplicity and data-independence is that a large number of random features is often needed to approximate the kernel matrix well [20, 22, 25, 33, 51].

The question naturally arises, then, as to whether we can combine the simplicity of random features and the ability to scale to large- p problems with the appealing approximation and statistical properties of Nyström-type approaches. We provide one possible solution by making random features data-dependent, and we show promising theoretical and empirical results. Our key insight is to begin with a large set of random features, then reduce them to a small set of weighted features in a data-dependent, computationally efficient way, while preserving the statistical guarantees of using the original large set. We frame the task of finding this small set of features as an optimization problem, which we solve using ideas from the coresets literature [5, 6]. Using greedy optimization schemes such as the Frank–Wolfe algorithm, we show that a large set of J_+ random features can be compressed to an *exponentially smaller* set of just $O(\log J_+)$ features while still achieving the same statistical guarantees as using all J_+ features. We demonstrate that our method achieves superior performance to existing approaches on a range of real datasets—including one with over 50 million observations—in terms of kernel matrix approximation and classification accuracy.

2 Preliminaries and related work

Suppose we observe data $\{(x_n, y_n)\}_{n=1}^N$ with predictors $x_n \in \mathbb{R}^p$ and responses $y_n \in \mathbb{R}$. In a supervised learning task, we aim to find a model $f : \mathbb{R}^p \rightarrow \mathbb{R}$ among a set of candidates \mathcal{F} that predicts the response well for new predictors. Modern data sets of interest often reach N in the tens of millions or higher, allowing analysts to learn particularly complex relationships in data. Nonparametric kernel methods [40] offer a flexible option in this setting; by taking \mathcal{F} to be a reproducing kernel Hilbert space with positive-definite kernel $k : \mathbb{R}^p \times \mathbb{R}^p \rightarrow \mathbb{R}$, they enable learning more nuanced details of the model f as more data are obtained. As a result, kernel methods are widespread not just in regression and classification but also in dimensionality reduction, conditional independence testing, one and two-sample testing, and more [10, 15, 16, 41, 54].

The problem, however, is that kernel methods become computationally intractable for large N . We consider kernel ridge regression as a prototypical example [39]. Let $K \in \mathbb{R}^{N \times N}$ be the kernel matrix consisting of entries $K_{nm} := k(x_n, x_m)$. Collect the responses into the vector $y \in \mathbb{R}^N$. Then kernel ridge regression requires solving

$$\min_{\alpha \in \mathbb{R}^N} -\frac{1}{2} \alpha^T (K + \lambda I) \alpha + \alpha^T y,$$

where $\lambda > 0$ is a regularization parameter. Computing and storing K alone has $O(N^2)$ complexity, while computing the solution $\alpha^* = (K + \lambda I)^{-1} y$ further requires solving a linear system, with cost $O(N^3)$. Many other kernel methods have $O(N^3)$ dependence; see Table 1.

To make kernel methods tractable on large datasets, a common practice is to replace the kernel matrix K with an approximate low-rank factorization $\hat{K} := ZZ^T \approx K$, where $Z \in \mathbb{R}^{N \times J}$ and $J \ll N$. This factorization can be viewed as replacing the kernel function k with a finite-dimensional inner product $k(x_n, x_m) \approx z(x_n)^T z(x_m)$ between features generated by a *feature map* $z : \mathbb{R}^p \rightarrow \mathbb{R}^J$. Using this type of approximation significantly reduces downstream training time, as shown in the second column of Table 1. Previous results show that as long as ZZ^T is close to K in the Frobenius norm, the optimal model f using \hat{K} is uniformly close to the one using K [11]; see the rightmost column of Table 1.

Table 1: A comparison of training time for PCA, SVM, and ridge regression using the exact kernel matrix K versus a low-rank approximation $\hat{K} = ZZ^T$, where Z has J columns. Exact training requires either inverting or computing the SVD of the true kernel matrix K at a cost of $O(N^3)$ time, as shown in the first column. The second column refers to training the methods using a low-rank factorization Z . For ridge regression and PCA, the low-rank training cost reflects the time to compute and invert the feature covariance matrix $Z^T Z$. For SVM, the time refers to fitting a linear SVM on Z using *dual-coordinate descent* with optimization tolerance ρ [21]. The third column quantifies the uniform error between the function fit using K and the function fit using Z . For specific details of how the bounds were derived, see Appendix D.

| Method | Exact Training Cost | Low-Rank Training Cost | Approximation Error |
|------------------|---------------------|----------------------------------|--|
| PCA | $O(N^3)$ | $\Theta(NJ^2)$ | $O\left(\left(1 - \frac{\ell}{N}\right)\ \hat{K} - K\ _F\right)$ |
| SVM | $O(N^3)$ | $\Theta(NJ \log \frac{1}{\rho})$ | $O\left(\ \hat{K} - K\ _F^{\frac{1}{2}}\right)$ |
| Ridge Regression | $O(N^3)$ | $\Theta(NJ^2)$ | $O\left(\frac{1}{N}\ \hat{K} - K\ _F\right)$ |

However, finding a good feature map is a nontrivial task. One popular method, known as *random Fourier features* (RFF) [33], is based on Bochner’s Theorem:

Theorem 2.1 ([37, p. 19]). *A continuous, stationary kernel $k(x, y) = \phi(x - y)$ for $x, y \in \mathbb{R}^p$ is positive definite with $\phi(0) = 1$ if and only if there exists a probability measure Q such that*

$$\begin{aligned} \phi(x - y) &= \int_{\mathbb{R}^p} e^{i\omega^T(x-y)} dQ(\omega) \\ &= \mathbb{E}_Q[\psi_\omega(x)\psi_\omega(y)^*], \quad \psi_\omega(x) := e^{i\omega^T x}. \end{aligned} \tag{1}$$

Theorem 2.1 implies that $z_{\text{complex}}(x) := (1/\sqrt{J})[\psi_{\omega_1}(x), \dots, \psi_{\omega_J}(x)]^T$, where $\omega_i \stackrel{\text{i.i.d.}}{\sim} Q$, provides a Monte-Carlo approximation of the true kernel function. As noted by Rahimi and Recht [34], the real-valued feature map $z(x) := (1/\sqrt{J})[\cos(\omega_1^T x + b_1), \dots, \cos(\omega_J^T x + b_J)]^T$, $b_j \stackrel{\text{unif.}}{\sim} [0, 2\pi]$ also yields an unbiased estimator of the kernel function; we use this feature map in what follows unless otherwise stated. The resulting $N \times J$ feature matrix Z yields estimates of the true kernel function with standard Monte-Carlo error rates of $O(1/\sqrt{J})$ uniformly on compact sets [33, 45]. The RFF methodology also applies quite broadly. There are well-known techniques for obtaining samples from Q for a variety of popular kernels such as the squared exponential, Laplace, and Cauchy [33], as well as extensions to more general *random feature maps* (RFMs), which apply to many types of non-stationary kernels [12, 25, 32].

The major drawback of RFMs is the $O(NJp)$ time and $O(NJ)$ memory costs associated with generating the feature matrix Z .¹ Although these are linear in N as desired, recent empirical evidence [22] suggests that J needs to be quite large to provide competitive performance with other data analysis techniques. Recent work addressing this drawback has broadly involved two approaches: *variance reduction* and *feature compression*. Variance reduction techniques involve modifying the standard Monte-Carlo estimate of k , e.g. with control variates, quasi-Monte-Carlo techniques, or importance sampling [1, 2, 8, 42, 53]. These approaches either depend poorly on the data dimension p (in terms of statistical generalization error), or, for a fixed approximation error, reduce the number of features J compared to RFM only by a constant. Feature compression techniques, on the other hand, involve two steps: (1) “up-projection,” in which the basic RFM methodology generates a large number J_+ of features—followed by (2) “compression,” in which those features are used to find a smaller number J of features while ideally retaining the kernel approximation error of the original J_+ features. Compact random feature maps [18] represent an instance of this technique in which compression is achieved using the Johnson–Lindenstrauss (JL) algorithm [23]. However, not only is the generation and storage of J_+ features prohibitively expensive for large datasets, JL compression is *data-independent* and leads to only a constant reduction in J_+ as we show in Appendix C (see summary in Table 2).

¹*Fast Food RFM* can reduce the computational cost of generating the feature matrix to $O(NJ \log p)$ by exploiting techniques from sparse linear algebra. For simplicity, we focus on RFM here, but we note that our method can also be used on top of Fast Food RFM in cases when p is large.

3 Random feature compression via coresets

In this section, we present an algorithm for approximating a kernel matrix $K \in \mathbb{R}^{N \times N}$ with a low-rank approximation $K \approx \hat{K} = ZZ^T$ obtained using a novel feature compression technique. In the up-projection step we generate J_+ random features, but only compute their values for a small, randomly-selected subset of $S \ll N^2$ datapoint pairs. In the compression step, we select a sparse, weighted subset of J of the original J_+ features in a sequential greedy fashion. We use the feature values on the size- S subset of all possible data pairs to decide, at each step, which feature to include and its weight. Once this process is complete, we compute the resulting weighted subset of J features on the whole dataset. We use this low-rank approximation of the kernel in our original learning problem. Since we use a sparse weighted feature subset for compression—as opposed to a general linear combination as in previous work—we do not need to compute all J_+ features for the whole dataset. This circumvents the expensive $O(NJ_+p)$ up-projection computation typical of past feature compression methods. In addition, we show that our greedy compression algorithm needs to output only $J = O(\log J_+)$ features—as opposed to past work, where $J = O(J_+)$ was required—while maintaining the same kernel approximation error provided by RFM with J_+ features. These results are summarized in Table 2 and discussed in detail in Section 3.2.

3.1 Algorithm derivation

Let $Z_+ \in \mathbb{R}^{N \times J_+}$, $J_+ > J$, be a fixed up-projection feature matrix generated by RFM. Our goal is to use Z_+ to find a compressed low-rank approximation $\hat{K} = ZZ^T \approx K$, $Z \in \mathbb{R}^{N \times J}$. Our approach is motivated by the fact that spectral 2-norm bounds on $K - \hat{K}$ provide uniform bounds on the difference between learned models using K and \hat{K} [11], as well as the fact that the Frobenius norm bounds the 2-norm. So we aim to find a Z that minimizes the Frobenius norm error $\|K - ZZ^T\|_F$. By the triangle inequality,

$$\begin{aligned} & \|K - ZZ^T\|_F \\ & \leq \|K - Z_+Z_+^T\|_F + \|Z_+Z_+^T - ZZ^T\|_F, \end{aligned} \quad (2)$$

so constructing a good feature compression down to J features amounts to picking Z such that $Z_+Z_+^T \approx ZZ^T$ in Frobenius norm. Let $Z_{+,j} \in \mathbb{R}^N$ denote the j th column of Z_+ . Then we would ideally like to solve the optimization problem

$$\begin{aligned} & \underset{w \in \mathbb{R}_+^{J_+}}{\operatorname{argmin}} \quad \frac{1}{N^2} \|Z_+Z_+^T - Z(w)Z(w)^T\|_F^2 \\ & \text{s.t. } Z(w) := \left[\sqrt{w_1}Z_{+,1} \quad \cdots \quad \sqrt{w_{J_+}}Z_{+,J_+} \right] \\ & \quad \|w\|_0 \leq J. \end{aligned} \quad (3)$$

This problem is intractable to solve exactly for two main reasons. First, computing the objective function requires computing Z_+ , which itself takes $\Omega(NJ_+p)$ time. But it is not uncommon for all three of N , J_+ , and p to be large, making this computation expensive. Second, the cardinality, or “0-norm,” constraint on w yields a difficult combinatorial optimization. In order to address these issues, first note that

$$\begin{aligned} & \frac{1}{N^2} \|Z_+Z_+^T - Z(w)Z(w)^T\|_F^2 = \\ & \mathbb{E}_{i,j \stackrel{\text{i.i.d.}}{\sim} \pi} \left[(z_{+,i}^T z_{+,j} - z_i(w)^T z_j(w))^2 \right], \end{aligned}$$

where π is the uniform distribution on the integers $\{1, \dots, N\}$, and $z_{+,i}, z_i(w) \in \mathbb{R}^{J_+}$ are the i th rows of $Z_+, Z(w)$, respectively. Therefore, we can generate a Monte-Carlo estimate of the optimization objective by sampling S pairs $i_s, j_s \stackrel{\text{i.i.d.}}{\sim} \pi$:

$$\begin{aligned} & \frac{S}{N^2} \|Z_+Z_+^T - Z(w)Z(w)^T\|_F^2 \\ & \approx \sum_{s=1}^S (z_{+,i_s}^T z_{+,j_s} - z_{i_s}(w)^T z_{j_s}(w))^2 \\ & = (1-w)^T R R^T (1-w) \text{ s.t.} \end{aligned} \quad (4)$$

$$R := [z_{+i_1} \circ z_{+j_1}, \dots, z_{+i_S} \circ z_{+j_S}] \in \mathbb{R}^{J_+ \times S},$$

where \circ indicates a component-wise product. Denoting the j th row of R by $R_j \in \mathbb{R}^S$ and the sum of the rows by $r = \sum_{j=1}^{J_+} R_j$, we can rewrite the Monte Carlo approximation of the original optimization problem in Eq. (3) as

$$\begin{aligned} & \underset{w \in \mathbb{R}_+^{J_+}}{\operatorname{argmin}} \quad \|r - r(w)\|_2^2 \\ & \text{s.t.} \quad \|w\|_0 \leq J, \end{aligned} \tag{5}$$

where $r(w) := \sum_{j=1}^{J_+} w_j R_j$. Note that the s^{th} component $r_s = z_{+i_s}^T z_{+j_s}$ of r is the Monte-Carlo approximation of $k(x_{i_s}, x_{j_s})$ using all J_+ features, while $r(w)_s = (\sqrt{w} \circ z_{+i_s})^T (\sqrt{w} \circ z_{+j_s})$ is the sparse Monte-Carlo approximation using weights $w \in \mathbb{R}_+^{J_+}$. In other words, the difference between the full optimization in Eq. (3) and the reformulated optimization in Eq. (5) is that the former attempts to find a sparse, weighted set of features that approximates the full J_+ -dimensional feature inner products for all data pairs, while the latter attempts to do so only for the subset of pairs i_s, j_s , $s \in \{1, \dots, S\}$. Since a kernel matrix is symmetric and $k(x_n, x_n) = 1$ for any datapoint x_n , we only need to sample (i, j) above the diagonal of the $N \times N$ matrix (see Algorithm 1).

The reformulated optimization problem in Eq. (5)—i.e., approximating the sum r of a collection $(R_j)_{j=1}^{J_+}$ of vectors in \mathbb{R}^S with a sparse weighted linear combination—is precisely the *Hilbert coreset construction problem* studied in previous work [5, 6]. There exist a number of efficient algorithms to solve this problem approximately; in particular, the Frank–Wolfe-based method of Campbell and Broderick [6] and “greedy iterative geodesic ascent” (GIGA) [5] both provide an exponentially decreasing objective value as a function of the compressed number of features J . Note that it is also possible to apply other more general-purpose methods for cardinality-constrained convex optimization [7, 9, 47], but these techniques are often too computationally expensive in the large-dataset setting. Our overall algorithm for feature compression is shown in Algorithm 1.

Algorithm 1 Random Feature Maps Compression (RFM-FW / RFM-GIGA)

Input: Data $(x_n)_{n=1}^N$ in \mathbb{R}^p , RFM distribution Q , number of starting random features J_+ , number of compressed features J , number of data pairs S

Output: Weights $w \in \mathbb{R}^{J_+}$ with at most J non-zero entries

- 1: $(i_s, j_s)_{s=1}^S \stackrel{\text{i.i.d.}}{\sim} \text{Unif}(\{(i, j) : i < j, 2 \leq j \leq N\})$.
 - 2: Sample $(\omega_j)_{j=1}^{J_+} \stackrel{\text{i.i.d.}}{\sim} Q$
 - 3: Sample $b_j \stackrel{\text{unif.}}{\sim} [0, 2\pi]$, $1 \leq j \leq J_+$
 - 4: **for** $s = 1 : S$ **do**
 - 5: Compute $z_{+i_s} \leftarrow (1/\sqrt{J_+})[\cos(\omega_1^T x_{i_s} + b_1), \dots, \cos(\omega_{J_+}^T x_{i_s} + b_{J_+})]^T$; same for z_{+j_s}
 - 6: Compute $R \leftarrow [z_{+i_1} \circ z_{+j_1}, \dots, z_{+i_S} \circ z_{+j_S}]$
 - 7: $R_j \leftarrow$ row j of R ; $r \leftarrow \sum_{j=1}^{J_+} R_j$
 - 8: $w \leftarrow$ solution to Eq. (5) with FW [6] or GIGA [5]
 - 9: $Z(w) = [\sqrt{w_1} Z_{+1} \quad \dots \quad \sqrt{w_{J_+}} Z_{+J_+}]$
 - 10: **return** $Z(w)$
-

3.2 Theoretical results

In order to employ Algorithm 1, we must choose the number S of data pairs, the up-projected feature dimension J_+ , and compressed feature dimension J . Selecting these three quantities involves a tradeoff between the computational cost of using Algorithm 1 and the resulting low-rank kernel approximation Frobenius error, but it is not immediately clear how to perform that tradeoff. Theorem 3.2 and Corollary 3.3 provide a remarkable resolution to this issue: roughly, if we fix J_+ such that the basic random features method provides kernel approximation error $\epsilon > 0$ with high probability, then choosing $S = \Omega(J_+^2 (\log J_+)^2)$ and $J = \Omega(\log J_+)$ suffices to guarantee that the compressed feature kernel approximation error is also $O(\epsilon)$ with high probability. In contrast, previous feature compression methods required $J = \Omega(J_+)$ to achieve the same result; see Table 2.

Table 2: A comparison of the computational cost of basic random feature maps (RFM), RFM with JL compression (RFM-JL), and RFM with our proposed compression using FW (RFM-FW) for N datapoints and $J_+ = 1/\epsilon \log 1/\epsilon$ up-projection features. The first column specifies the number of compressed features J needed to retain the $O(\epsilon)$ high probability kernel approximation error guarantee of RFM. The second and third columns list the complexity for computing the compressed features and using them for PCA or ridge regression, respectively. Theoretically, the number of datapoint pairs S should be set to $\Omega(J_+^2 (\log J_+)^2)$ in Algorithm 1 (see Theorem 3.2) but empirically we find in Section 4 that S can be set much smaller. See Appendix C for derivations.

| Method | # Compressed Features J | Cost of Computing Z | PCA/Ridge Reg. Cost |
|--------|---------------------------|---------------------------------|---------------------|
| RFM | $O(J_+)$ | $O(NJ_+)$ | $O(NJ_+^2)$ |
| RFM-JL | $O(J_+)$ | $O(NJ_+ \log J_+)$ | $O(NJ_+^2)$ |
| RFM-FW | $O(\log J_+)$ | $O(SJ_+ \log J_+ + N \log J_+)$ | $O(N(\log J_+)^2)$ |

Note that Theorem 3.2 assumes that the compression step in Algorithm 1 is completed using the Frank–Wolfe-based method from Campbell and Broderick [6]. However, this choice was made solely to simplify the theory; as GIGA [5] provides stronger performance both theoretically and empirically, we expect a stronger result than Theorem 3.2 and Corollary 3.3 to hold when using GIGA. The proof of Theorem 3.2 is given in Appendix B and depends on the following assumptions.

Assumption 3.1. (a) The cardinality of the set of vectors $\{x_i - x_j, x_i + x_j\}_{1 \leq i < j \leq N}$ is $\frac{N(N-1)}{2}$, i.e., all vectors $x_i - x_j, x_i + x_j, 1 \leq i < j \leq N$ are distinct.

(b) $Q(\omega)$ for $\omega \in \mathbb{R}^p$ has strictly positive density on all of \mathbb{R}^p , where Q is the measure induced by the kernel k ; see Theorem 2.1.

Assumption 3.1(a-b) are sufficient to guarantee that the compression coefficient ν_{J_+} provided in Theorem 3.2 does not go to 1. If $\nu_{J_+} \rightarrow 1$ as $J_+ \rightarrow \infty$, the amount of compression could go to zero asymptotically. When the x_j 's contain continuous (noisy) measurements, Assumption 3.1(a) is very mild since the difference or sum between two datapoints is unlikely to equal the difference or sum between two other datapoints. Assumption 3.1(b) is satisfied by most kernels used in practice (e.g. radial basis function, Laplace kernel, etc.).

We obtain the exponential compression in Theorem 3.2 for the following reason: Frank-Wolfe and GIGA converge linearly when the minimizer of Eq. (5) belongs to the relative interior of the feasible set of solutions [29], which turns out to occur in our case. With linear convergence, we need to run only a *logarithmic* number of iterations (which upper bounds the sparsity of w) to approximate r by $r(w)$ for a given level of approximation error. For fixed J_+ , Lemma A.5 from Campbell and Broderick [6] immediately implies that the minimizer belongs to the relative interior. As $J_+ \rightarrow \infty$ (that is, as we represent the kernel function exactly), we show that the minimizer asymptotically belongs to the relative interior, and we provide a lower bound on its distance to the boundary of the feasible set. This distance lower bound is key to the asymptotic worst-case bound on the compression coefficient given in Theorem 3.2 and Theorem 3.4.

Theorem 3.2. Fix $\epsilon > 0$, $\delta \in (0, 1)$, and $J_+ \in \mathbb{N}$. Then there are constants $\nu_{J_+} \in (0, 1)$, which depends only on J_+ , and $0 \leq c_\delta^* < \infty$, which depends only on δ , such that if

$$J = \Omega\left(-\frac{\log J_+}{\log \nu_{J_+}}\right) \text{ and } S = \Omega\left(\frac{c_\delta^*}{\epsilon^2} \left[\frac{\log \frac{1}{\epsilon}}{\log \nu_{J_+}}\right]^4 \log J_+\right),$$

then with probability at least $1 - \delta$, the output Z of Algorithm 1 satisfies

$$\frac{1}{N^2} \|Z_+ Z_+^T - Z Z^T\|_F^2 \leq \epsilon.$$

Furthermore, the compression coefficient is asymptotically bounded away from 1. That is,

$$0 < \limsup_{J_+ \rightarrow \infty} \nu_{J_+} < 1. \quad (6)$$

Corollary 3.3. In the setting of Theorem 3.2, if we let $J_+ = \Omega(1/\epsilon \log 1/\epsilon)$, then

$$\frac{1}{N^2} \|K - Z Z^T\|_F^2 = O(\epsilon).$$

Proof. Claim 1 of Rahimi and Recht [33] implies that $\frac{1}{N^2} \|K - Z_+ Z_+^T\|_F^2 = O(\epsilon)$ if we set $J_+ = \Omega(1/\epsilon \log 1/\epsilon)$. The result follows by combining Theorem 3.2 and Eq. (2). \square

Table 2 builds on the results of Theorem 3.2 and Corollary 3.3 to illustrate the benefit of our proposed feature compression technique in the settings of kernel principal component analysis (PCA) and ridge regression. Since random features and random features with JL compression both have $J = \Omega(J_+)$, the $O(NJ_+^2)$ cost of computing the feature covariance matrix $Z^T Z$ dominates when training PCA or ridge regression. In contrast, the dominant cost of random features with our proposed algorithm is the compression step; each iteration of Frank-Wolfe has cost $O(J_+ S)$, and we run it for $O(\log J_+)$ iterations.

While Corollary 3.3 says how large S must be for a given J_+ , it does not say how to pick J_+ , or equivalently how to choose the level of precision ϵ . As one would expect, the amount of precision needed depends on the downstream application. For example, recent theoretical work suggests that both kernel PCA and kernel ridge regression require J_+ to scale only sublinearly with the number of datapoints N to achieve the same statistical guarantees as an exact kernel machine trained on all N datapoints [2, 35, 43]. For kernel support vector machines (SVMs), on the other hand, Sutherland and Schneider [45] suggest that J_+ needs to be larger than N . Such a choice of J_+ would make random features *slower* than training an exact kernel SVM. However, since Sutherland and Schneider [45] do not provide a lower bound, it is still an open theoretical question how J_+ must scale with N for kernel SVMs.

For J_+ even moderately large, setting $S = \Omega(J_+^2 (\log J_+)^2)$ to satisfy Theorem 3.2 will be prohibitively expensive. Fortunately, in practice, we find $S \ll J_+^2$ suffices to provide significant practical computational gains without adversely affecting approximation error; see the results in Section 4. We conjecture that we see this behavior since we expect even a small number of data pairs S to be enough to guide feature compression in a data-dependent manner. We empirically verify this intuition in Fig. 4 of Section 4.

Finally, we provide an asymptotic upper bound for the compression coefficient ν_{J_+} . We achieve greater compression when $\nu_{J_+} \downarrow 0$. Hence, the upper bound below shows the asymptotic worst-case rate of compression.

Theorem 3.4. *Suppose all $\{(i, j) : 1 \leq i < j \leq N\}$ are sampled in Algorithm 1. Then,*

$$0 < \limsup_{J_+ \rightarrow \infty} \nu_{J_+} < 1 - \frac{\left(1 - \frac{\|K\|_F}{c_Q}\right)^2}{2} < 1, \quad (7)$$

where K is the exact kernel matrix and

$$c_Q := \frac{1}{N} \mathbb{E}_{\omega \sim Q, b \sim \text{Unif}[0, 2\pi]} \|u(\omega, b)\|_2, \text{ with} \quad (8)$$

$$u(\omega, b) := (\cos(\omega^T x_i + b) \cos(\omega^T x_j + b))_{i, j \in [N]}.$$

By Theorem 2.1, $\|K\|_F = \frac{1}{N} \mathbb{E}_{\omega, b} \|u(\omega, b)\|_2$, so $\|K\|_F \leq c_Q$ by Jensen’s inequality. In Appendix A, we show this inequality holds strictly. Hence the term squared in Eq. (7) lies in $(0, 1]$. Recall $\|K\|_F^2 = \sum_{i=1}^N \lambda_i$, for λ_i the eigenvalues of K . With these observations, Theorem 3.4 says that the asymptotic worst-case rate of compression improves if K ’s eigenvalue sum is smaller. As rough intuition: If the sum is small, then K may be nearly low-rank and thus easier to approximate via a low-rank approximation. Since we subsample only S of all pairs in Theorem 3.2, the upper bound in Theorem 3.4 does not necessarily apply. Nonetheless, for S moderately large, this upper bound roughly characterizes the worst-case compression rate for Algorithm 1.

4 Experiments

In this section we provide an empirical comparison of basic random feature maps (RFM) [33], RFM with Johnson-Lindenstrauss compression (RFM-JL) [18], and our proposed algorithm with compression via greedy iterative geodesic ascent [5] (RFM-GIGA). We note that there are many other random feature methods, such as Quasi-Monte-Carlo random features [1], that one might consider besides RFM-JL. A strength of our method is that it can be used as an additional compression step

Table 3: All datasets are taken from LIBSVM.

| Dataset | # Samples | Dimension | # Classes |
|------------|------------|-----------|-----------|
| Adult | 48,842 | 123 | 2 |
| Human | 10,299 | 561 | 6 |
| MNIST | 70,000 | 780 | 10 |
| Sensorless | 58,000 | 9 | 11 |
| Criteo | 51,882,752 | 1,000,000 | 2 |

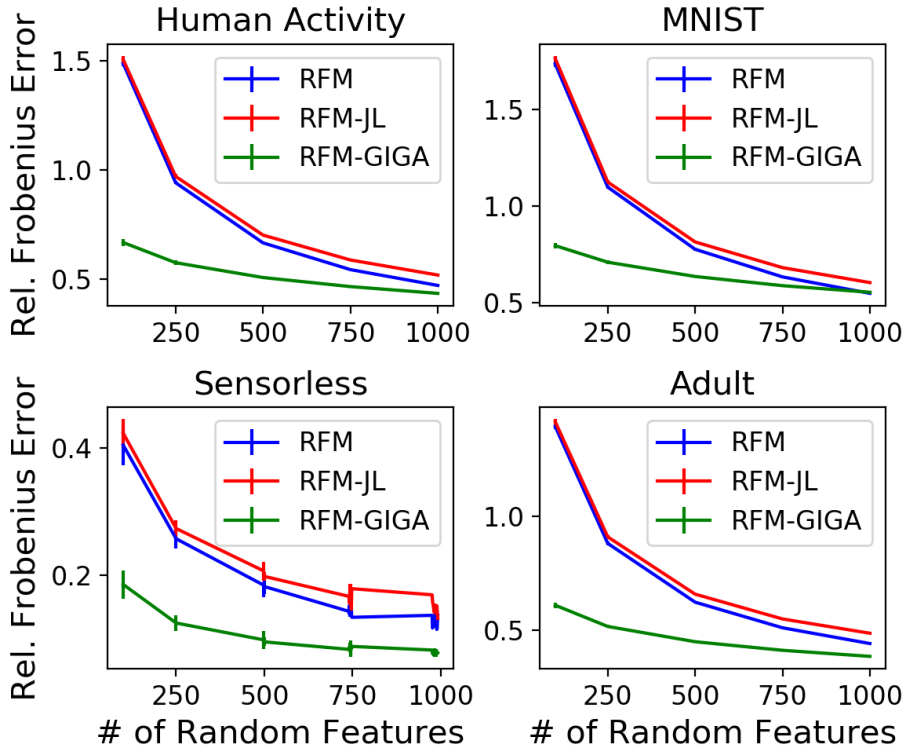


Figure 1: Kernel matrix approximation error. Lower is better. Points average 20 runs; error bar is one standard deviation.

with these methods and is thus complementary with them; we discuss this idea and demonstrate the resulting improvements in Appendix E. In this section, we focus on Johnson-Lindenstrauss as the current state-of-the-art random features compression method.

We compare performance on the task of kernel SVM classification [49]. We consider five real, large-scale datasets, summarized in Table 3. We assess performance via two quality metrics—Frobenius error of the kernel approximation and test set classification error. We also measure overall computation time—including both random feature projection and SVM training. We use the radial basis kernel $k(x, y) = e^{-\gamma\|x-y\|^2}$; we pick both γ and the SVM regularization strength for each dataset by randomly sampling 10,000 datapoints, training an exact kernel SVM on those datapoints, and using 5-fold cross-validation. For both RFM-JL and RFM-GIGA we set $J_+ = 5,000$, and for RFM-GIGA we set $S = 20,000$.

Figs. 1 and 2 show the relative kernel matrix approximation error $\|ZZ^T - K\|_F/\|K\|_F$ and test classification accuracy, respectively, as a function of the number of compressed features J . Note that, since we cannot actually compute K , we approximate the relative Frobenius norm error by randomly sampling 10^4 datapoints. We ran each experiment 20 times; the results in Figs. 1 and 2 show the mean across these trials with one standard deviation denoted with error bars. RFM-GIGA outperforms RFM and RFM-JL across all the datasets, on both metrics, for the full range of number of compressed features that we tested. This empirical result corroborates the theoretical results presented earlier in

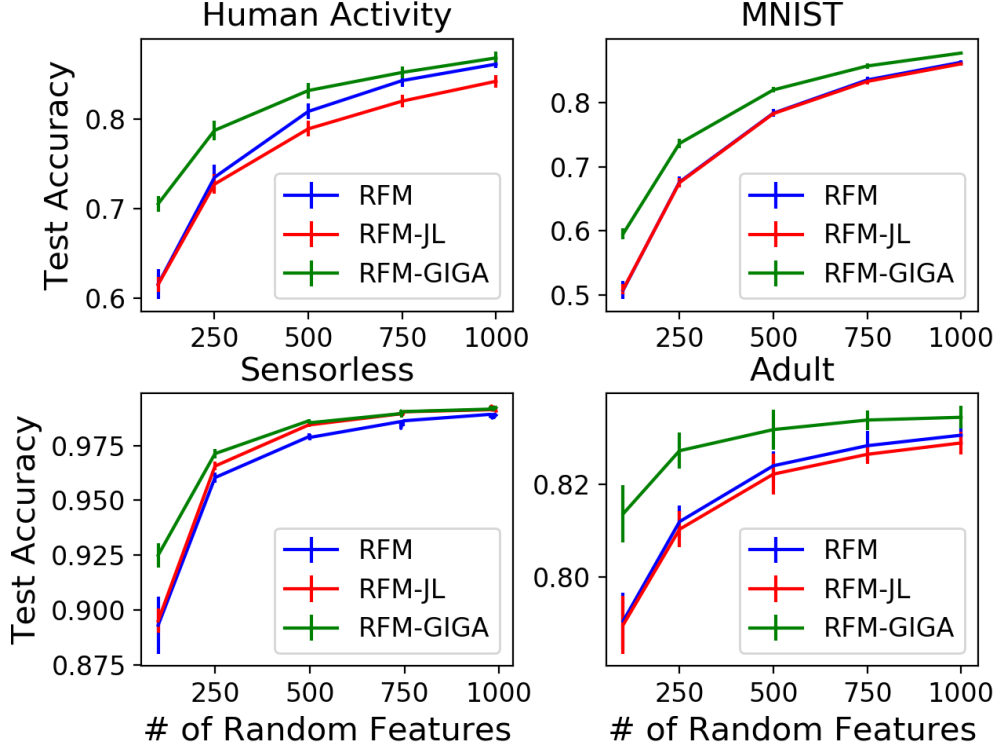


Figure 2: Classification accuracy. Higher is better. Points average 20 runs; error bar is one standard deviation.

Section 3.2; in practice, RFM-GIGA requires approximately an order of magnitude fewer features than either RFM or RFM-JL.

To demonstrate the computational scalability of RFM-GIGA, we also plot the relative kernel matrix approximation error versus computation time for the Criteo dataset, which consists of over 50 million data points. Before random feature projection and training, we used sparse random projections [27] to reduce the input dimensionality to 250 dimensions (due to memory constraints). We set $J_+ = 5000$ and $S = 2 \times 10^4$ as before, and let J vary between 10^2 and 10^3 . The results of this experiment in Fig. 3 suggest that RFM-GIGA provides a significant improvement in performance over both RFM and RFM-JL. Note that RFM-JL is very expensive in this setting—the up-projection step requires computing a 5×10^8 by 5×10^3 feature matrix—explaining its large computation time relative to RFM and RFM-GIGA. For test-set classification, all the methods performed the same for all choices of J (accuracy of 0.74 ± 0.001), so we do not provide the runtime vs. classification accuracy plot. This result is likely due to our compressing the 10^6 -dimensional feature space to 250 dimensions, making it hard for the SVM classifier to properly learn.

Given the empirical advantage of our proposed method, we next focus on understanding (1) if S can be set much smaller than $\Omega(J_+^2(\log J_+)^2)$ in practice and (2) if we can get an exponential compression of J_+ in practice as Theorem 3.2 and Theorem 3.4 guarantee.

To test the impact of S on performance, we fixed $J_+ = 5,000$, and we let S vary between 10^2 and 10^6 . Figure 4 shows what the results in Fig. 1 would have looked like had we chosen a different S . We clearly see that after around only $S = 10,000$ there is a phase transition such that increasing S does not further improve performance.

To better understand if we actually see an exponential compression in J_+ in practice, as our theory suggests, we set $J_+ = 10^5$ (i.e. very large) and fixed $S = 20,000$ as before. We examined the HIGGS dataset consisting of 1.1×10^7 samples, and let J (the number of compressed features) vary between 500 and 10^4 . Since GIGA can select the same random feature at different iterations (i.e. give a feature higher weight), J reached 8,600 after 10^4 iterations in Fig. 5. Fig. 5 shows that for $J \approx 2 \times 10^3$, increasing J further has negligible impact on kernel approximation performance—only

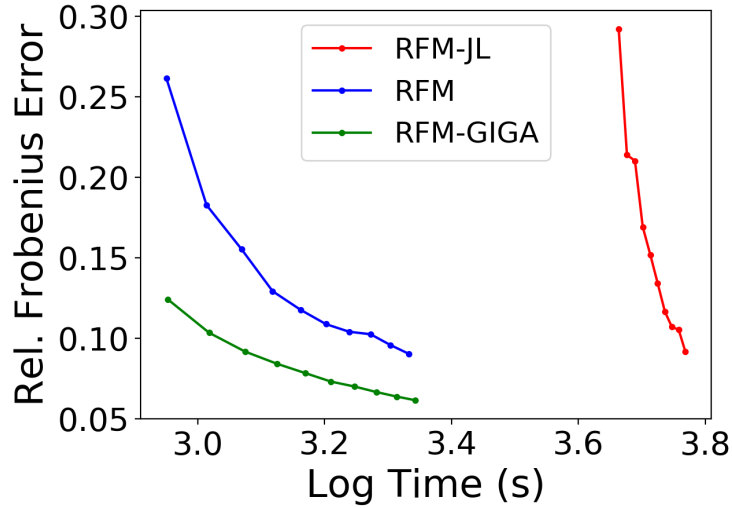


Figure 3: Log clock time vs. kernel matrix approximation quality on the Criteo data. Lower is better.

0.001 difference in relative error. Fig. 5 shows that we are able to compress J_+ by around two orders of magnitude.

Finally, since our proofs of Theorem 3.2 and Theorem 3.4 assume Step 8 of Algorithm 1 is run using Frank-Wolfe instead of GIGA, we compare in Fig. 6 how the results in Fig. 1 change by using Frank-Wolfe instead. Fig. 6 shows that for J small, GIGA has better approximation quality than FW but for larger J , the two perform nearly the same. This behavior agrees with the theory and empirical results of Campbell and Broderick [5], where GIGA is motivated specifically for the case of high compression.

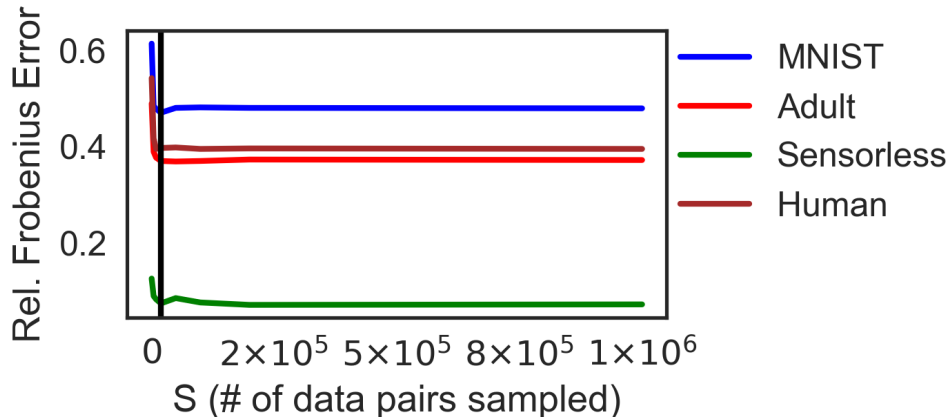


Figure 4: We plot the relative Frobenius norm error against S for J_+ fixed at 5,000. The solid black line corresponds to the results found in Fig. 1.

5 Conclusion

This work presents a new algorithm for scalable kernel matrix approximation. We first generate a low-rank approximation. We then find a sparse, weighted subset of the columns of the low-rank factor that minimizes the Frobenius norm error relative to the original low-rank approximation. Theoretical and empirical results suggest that our method provides a substantial improvement in scalability and approximation quality over past techniques. Directions for future work include investigating the effects of variance reduction techniques for the up-projection, using a similar compression technique

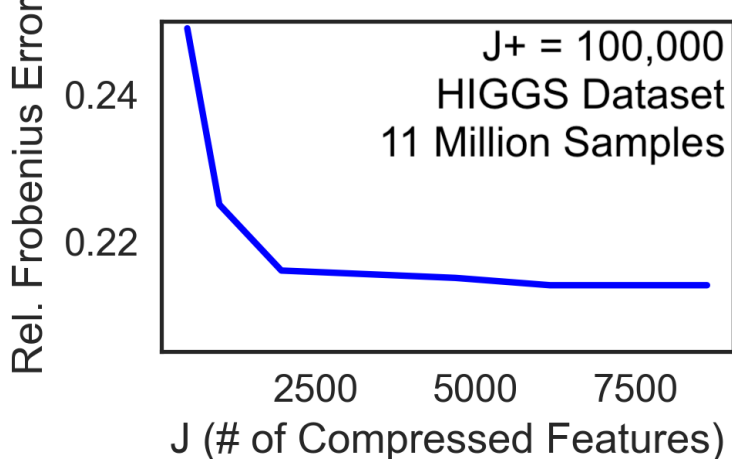


Figure 5: Let $S = 20,000$, $J_+ = 10^5$. We plot the relative Frobenius norm error vs. J from 500 to 10^4 .

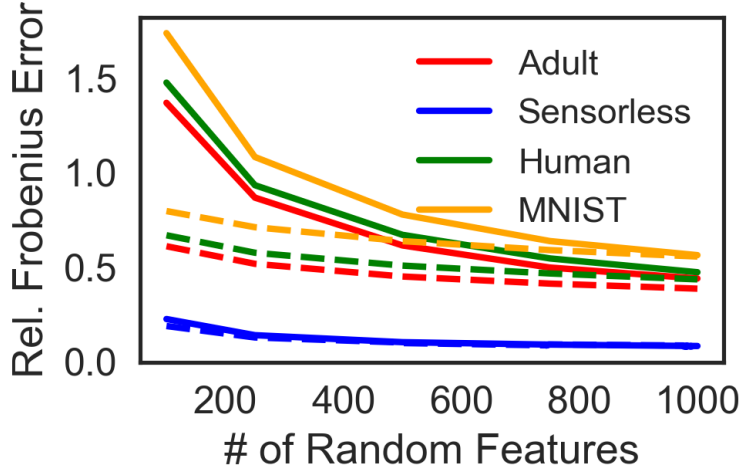


Figure 6: The performance of GIGA versus Frank-Wolfe for the experiment described in Fig. 1. Solid lines correspond to Frank-Wolfe and dashed with GIGA.

on features generated by the Nyström method [50], and transfer learning of feature weights for multiple related datasets.

Acknowledgments

We thank Justin Solomon for valuable discussions. This research was supported in part by an ARO YIP Award, ONR (N00014-17-1-2072), an NSF CAREER Award, the CSAIL-MIT Trustworthy AI Initiative, Amazon, and the MIT-IBM Watson AI Lab.

A Proof of Theorem 3.4

The proofs of Theorem 3.2 and Theorem 3.4 rely on the main error bound for the *Hilbert coreset construction problem* given in Eq. (9) [6]. We restate this error bound in Lemma A.2, which depends on several key quantities given below:

- $c_{ls} := \frac{1}{J_+} \cos(\omega_l^T x_{i_s} + b_l) \cos(\omega_l^T x_{j_s} + b_l)$, such that $1 \leq s \leq S$ and $1 \leq l \leq J_+$
- $\hat{\sigma}_j^2 := \frac{1}{S} \sum_{s=1}^S c_{js}^2 = \frac{1}{S} \|R_j\|_2^2$

- $\hat{\sigma}^2 := \left(\sum_{j=1}^{J_+} \hat{\sigma}_j \right)^2$

Definition A.1. [6] The *Hilbert construction problem* is based on solving the quadratic program,

$$\operatorname{argmin}_{w \in \mathbb{R}_+^{J_+}} \frac{1}{S} \|r - r(w)\|_2^2 \quad \text{s.t.} \quad \sum_{j=1}^{J_+} w_j \hat{\sigma}_j = \hat{\sigma}. \quad (9)$$

Remark. The minimizer of Eq. (9) is $w^* = (1, \dots, 1)$ since $r(w^*) = r$. However, the goal is to find a sparse w . Instead of adding sparsity-inducing constraints (such as L_1 penalties), which would lead to computational difficulties for large-scale problems, Campbell and Broderick [6] minimize Eq. (9) greedily through the Frank-Wolfe algorithm. Frank-Wolfe outputs a sparse w since the sparsity of w is bounded by the number of iterations Frank-Wolfe is run for.

Lemma A.2. [6, Theorem 4.4] Solving Eq. (9) with J iterations of Frank-Wolfe satisfies

$$\begin{aligned} \frac{1}{S} \|r - r(w)\|_2^2 &\leq \frac{\hat{\sigma}^2 \eta^2 \bar{\eta}^2 \nu_J^2}{\bar{\eta}^2 \nu^{-2(J-2)} + \eta^2 (J-1)} \\ &\leq \nu_J^{2J-2}, \end{aligned} \quad (10)$$

where $0 \leq \nu_J < 1$. Furthermore, $\nu_J^2 = 1 - \frac{d^2}{\sigma^2 \bar{\eta}^2}$ where d is the distance from r to the nearest boundary of the convex hull of $\left\{ \frac{\hat{\sigma}}{\hat{\sigma}_j} R_j \right\}_{j=1}^{J_+}$ and $\bar{\eta}^2 := \frac{1}{S} \max_{i,j \in [J_+]} \left\| \frac{R_i}{\hat{\sigma}_i} - \frac{R_j}{\hat{\sigma}_j} \right\|^2$, $0 \leq \bar{\eta} \leq 2$.

We prove Theorem 3.4 first since the main idea is captured in this proof. The proof of Theorem 3.2 is more involved since we must use a number of concentration bounds to justify subsampling only S datapoint pairs instead of all $\frac{N(N-1)}{2}$ possible datapoint pairs. Both proofs will also depend on the following constants.

- $\sigma_j^2 := \frac{1}{V^*} \sum_{s=1}^{V^*} c_{js}^2 = \frac{1}{V^*} \|R_j\|_2^2$
- $\sigma^2 := \left(\sum_{j=1}^{J_+} \sigma_j \right)^2$

Here, $V^* = \frac{N(N-1)}{2}$, that is when all datapoint pairs above the diagonal are included. $\hat{\sigma}_j^2$ and $\hat{\sigma}^2$ are simply unbiased estimates of σ_j^2 and σ^2 based on sampling only S instead of all V^* datapoint pairs.

While Lemma A.2 guarantees $0 < \nu_{J_+} < 1$, it does not guarantee that $\nu_{J_+} \rightarrow 1$ as the number of random features $J_+ \rightarrow \infty$. The following Lemma is critical in showing that ν_{J_+} does not approach 1, which would result in no compression.

Lemma A.3. Let $\{x_i\}_{i=1}^K$ be a set of points in \mathbb{R}^p that satisfies Assumption 3.1(a). Consider the vector $v_{\omega,b} = (\cos(\omega^T x_i + b) \cos(\omega^T x_j + b))_{i < j, i \in [K-1]} \in \mathbb{R}^{\frac{K(K-1)}{2}}$. Let the unit vector $u_{\omega,b} := \frac{v_{\omega,b}}{\|v_{\omega,b}\|}$. If $\omega_j \stackrel{i.i.d.}{\sim} F$ and $b_j \stackrel{i.i.d.}{\sim} G$, where F has positive density on all of \mathbb{R}^p and G has positive density on $[0, 2\pi]$, then

$$\begin{aligned} d\left(\operatorname{ConvexHull}\{u_{\omega_j, b_j}\}_{j=1}^J, \mathcal{S}^{\frac{K(K-1)}{2}-1}\right) &\rightarrow 0 \quad \text{for } J \rightarrow \infty \\ \text{s.t. } d(A, B) &:= \max_{a \in A, b \in B} \|a - b\|_2. \end{aligned} \quad (11)$$

Here, $\mathcal{S}^{\frac{K(K-1)}{2}-1}$ denotes the surface of the unit sphere in $\mathbb{R}^{\frac{K(K-1)}{2}}$.

Proof. By construction, each unit vector $u_i := u_{\omega_i, b_i}$ lies on the boundary of the unit sphere in $\mathbb{R}^{\frac{K(K-1)}{2}}$. Hence, F, G induce a distribution on $\mathcal{S}^{\frac{K(K-1)}{2}-1}$. It suffices to show $\mathcal{S}^{\frac{K(K-1)}{2}-1}$ has strictly positive density everywhere since, as $J \rightarrow \infty$, any arbitrarily small neighborhood around a collection of points that cover $\mathcal{S}^{\frac{K(K-1)}{2}-1}$ will be hit by some u_i with probability 1. By standard convexity arguments, the convex hull of the u_i will arbitrarily approach $\mathcal{S}^{\frac{K(K-1)}{2}-1}$ by taking the radius of the neighborhoods to zero. We now show $\mathcal{S}^{\frac{K(K-1)}{2}-1}$ has strictly positive density everywhere. Since u_i is the normalized vector of $v_i := v_{\omega_i, b_i}$ and each component of v_i is between

-1 and 1 , it suffices to show, by the continuity of the cosine function, that for any $a \in \{-1, 1\}^{\frac{K(K-1)}{2}}$ there exist some ω_i, b_i such that $\text{sign}(v_i) := (\text{sign}(v_{il}))_{l \in \frac{K(K-1)}{2}}$ equals a . Recall that

$$\cos(a) \cos(b) = \frac{1}{2}(\cos(a+b) + \cos(a-b)). \quad (12)$$

Take $b_i = 0$. Then, Equation (12) implies $v_{il} = \frac{1}{2}(\cos(\omega_i^T(x_{i_l} + x_{j_l})) + \cos(\omega_i^T(x_{i_l} - x_{j_l})))$. Consider the vector $\tilde{v}_i = (\cos(\omega_i^T(x_{i_l} + x_{j_l})), \cos(\omega_i^T(x_{i_l} - x_{j_l})))_{l \in \frac{K(K-1)}{2}} \in \mathbb{R}^{K(K-1)}$. It suffices to show that for any $\tilde{a} \in \{-1, 1\}^{K(K-1)}$, there exists an ω_i such that $\text{sign}(\tilde{v}_i) = \tilde{a}$. Recall that the cosine function has infinite *VC dimension*, namely that for any labeling $y_1, \dots, y_M \in \{-1, 1\}$ of distinct points $x_1, \dots, x_M \in \mathbb{R}^p$, there exists an ω^* such that $\text{sign}(\cos((\omega^*)^T x_m)) = y_m$. Take $M = K(K-1)$, $y_m = \tilde{a}_m$, $x_m = x_{i_m} + x_{j_m}$, and $x_{m+1} = x_{i_m} - x_{j_m}$. Since all the x_m are distinct by Assumption 3.1(a), we can find an ω_i such that $\text{sign}(\tilde{v}_i) = \tilde{a}$ as desired. \square

We now prove Theorem 3.4.

Proof. Each $R_j \in \mathbb{R}^{\frac{N(N-1)}{2}}$ and the R_j 's are i.i.d. since each ω_j is drawn i.i.d. from Q . The induced Hilbert norm $\|\cdot\|_H$ of each R_j is given by $\|R_j\|_H^2 = \frac{2}{N(N-1)}\|R_j\|_2^2$ [6]. Hence, $\tilde{R}_j := \frac{R_j}{\sigma_j}$ is a unit vector in the vector space with norm $\|\cdot\|_H$. By Lemma A.3,

$$d\left(\text{ConvexHull}\{\tilde{R}_j\}_{j=1}^{J_+}, \mathcal{S}^{\frac{N(N-1)}{2}-1}\right) \rightarrow 0 \quad (13)$$

Let $\tilde{r} := \frac{1}{\sigma} \sum_{j=1}^{J_+} \sigma_j \tilde{R}_j \in \text{ConvexHull}\{\tilde{R}_j\}_{j=1}^{J_+}$ and observe that $\tilde{r} = \frac{r}{\sigma}$. The distance, which we denote as d_{J_+} , between \tilde{r} and the $\text{ConvexHull}\{\tilde{R}_j\}_{j=1}^{J_+}$ approaches $1 - \|\tilde{r}\|_H$ since the $\text{ConvexHull}\{\tilde{R}_j\}_{j=1}^{J_+}$ approaches $\mathcal{S}^{\frac{N(N-1)}{2}-1}$. Hence,

$$\lim_{J_+ \rightarrow \infty} d_{J_+} = 1 - \lim_{J_+ \rightarrow \infty} \|\tilde{r}\|_H = 1 - \frac{\lim_{J_+ \rightarrow \infty} \|r\|_H}{\lim_{J_+ \rightarrow \infty} \sigma}. \quad (14)$$

Now,

$$r_s = \frac{1}{J_+} \sum_{j=1}^{J_+} c_{js} \xrightarrow{J_+ \rightarrow \infty} k(x_{i_s}, x_{j_s}). \quad (15)$$

Hence, as $J_+ \rightarrow \infty$,

$$\|r\|_H \rightarrow \sqrt{\frac{2}{N(N-1)} \sum_{i < j} (k(x_i, x_j))^2}. \quad (16)$$

Now,

$$\begin{aligned} \sigma &= \sum_{j=1}^{J_+} \sigma_j \\ &= \sum_{j=1}^{J_+} \sqrt{\frac{1}{V^*} \sum_{s=1}^{V^*} c_{js}^2} \\ &= \sum_{j=1}^{J_+} \sqrt{\frac{1}{V^*} \sum_{s=1}^{V^*} \frac{1}{J_+^2} \cos^2(\omega_j^T x_{i_s} + b_j) \cos^2(\omega_j^T x_{j_s} + b_j)} \\ &= \frac{1}{J_+} \sum_{j=1}^{J_+} \sqrt{\frac{1}{V^*} \sum_{s=1}^{V^*} \cos^2(\omega_j^T x_{i_s} + b_j) \cos^2(\omega_j^T x_{j_s} + b_j)} \\ &= \sqrt{\frac{2}{N(N-1)}} \frac{1}{J_+} \sum_{j=1}^{J_+} \|(\cos(\omega_j^T x_m + b_j) \cos(\omega_j^T x_n + b_j))_{m < n}\|_2 \\ &\rightarrow \sqrt{\frac{2}{N(N-1)}} \mathbb{E}_{\omega, b} \|(\cos(w^T x_m + b) \cos(w^T x_n + b))_{m < n}\|_2 \end{aligned} \quad (17)$$

If $x \neq y$ and $w \neq 0$, then

$$\begin{aligned} k(x, y) &= \mathbb{E}_{\omega, b} \cos(w^T x + b) \cos(w^T y + b) \\ &< \mathbb{E}_{\omega, b} |\cos(w^T x + b) \cos(w^T y + b)|. \end{aligned} \quad (18)$$

by Jensen's inequality. Hence, Eq. (18) and Assumption 3.1(a-b) together imply

$$\frac{\lim_{J_+ \rightarrow \infty} \|r\|_2}{\lim_{J_+ \rightarrow \infty} \sigma} < 1. \quad (19)$$

By Eq. (16) and Eq. (17),

$$\frac{\lim_{J_+ \rightarrow \infty} \|r\|_H}{\lim_{J_+ \rightarrow \infty} \sigma} \leq \frac{\|K\|_F}{\mathbb{E}_{\omega, b} \|u(\omega, b)\|_2}, \quad (20)$$

where $u(\omega, b)$ is defined in Theorem 3.4. Lemma A.2 says that $\nu_{J_+}^2 = 1 - \frac{d^2}{\sigma^2 \bar{\eta}^2}$, where d is the distance from r to the nearest boundary of the convex hull of $\left\{ \frac{\sigma}{\sigma_j} R_j \right\}_{j=1}^{J_+}$. Hence, $d = \sigma d_{J_+}$ and $\nu_{J_+}^2 = 1 - \frac{d_{J_+}^2}{\bar{\eta}^2}$. Eq. (14) and Eq. (20) together imply,

$$\liminf_{J_+ \rightarrow \infty} d_{J_+} \leq 1 - \frac{\|K\|_F}{\mathbb{E}_{\omega, b} \|u(\omega, b)\|_2}. \quad (21)$$

Therefore, since $0 \leq \bar{\eta}^2 \leq 2$ by Lemma A.2,

$$\begin{aligned} \limsup_{J_+ \rightarrow \infty} \nu_{J_+}^2 &\leq \limsup_{J_+ \rightarrow \infty} 1 - \frac{d_{J_+}^2}{2} \\ &= 1 - \liminf_{J_+ \rightarrow \infty} \frac{d_{J_+}^2}{2} \\ &\leq 1 - \frac{\left(1 - \frac{\|K\|_F}{\mathbb{E}_{\omega, b} \|u(\omega, b)\|_2}\right)^2}{2}. \end{aligned} \quad (22)$$

□

B Proof of Theorem 3.2

The following technical lemma is needed to derive the probability bound in Theorem 3.2.

Lemma B.1. Suppose $\frac{\sigma^2}{J_+^2 \sigma_i^2} \leq M$ for some $1 \leq M < \infty$ for all $i \in [J_+]$. For $S \geq 8 \frac{M^2}{\sigma^4} \log \left(\frac{2J_+}{\delta^2} \right)$

$$\mathbb{P} \left(\frac{\hat{\sigma}^2}{J_+^2 \hat{\sigma}_i^2} \geq 5M \right) \leq \delta \quad (23)$$

for all $i \in [J_+]$.

Proof. Notice that

$$\begin{aligned} \mathbb{E}_{i_s, j_s} \hat{\sigma}_l^2 &= \frac{1}{S} \sum_{s=1}^S \mathbb{E}_{i_s, j_s} c_{l_s}^2 \\ &= \frac{1}{N^2} \sum_{s=1}^{N^2} c_{l_s}^2 \\ &= \sigma_l^2. \end{aligned}$$

Hence, $\hat{\sigma}_l^2$ is an unbiased estimator of σ_l^2 . Each $c_{l_s}^2 \leq \frac{1}{J_+^2}$ is a bounded random variable, and the collection of random variables $\{c_{l_s}^2\}_{s=1}^S$ are i.i.d. since $i_s, j_s \stackrel{\text{i.i.d.}}{\sim} \pi$. Hence, by Hoeffding's inequality,

$$\mathbb{P} (|\hat{\sigma}_l^2 - \sigma_l^2| \geq t) \leq 2 \exp(-2SJ_+^4 t^2). \quad (24)$$

Define the event $A_t := \cup_{i=1}^{J_+} \{|\hat{\sigma}_i^2 - \sigma_i^2| < t\}$ and pick t such that $t \leq \min_{i \in [J_+]} \sigma_i^2$. Since $\sigma_i^2 \geq \frac{\sigma^2}{M}$ by assumption, it suffices to pick $0 < t \leq \frac{\sigma^2}{M}$. Conditioned on A_t , $\hat{\sigma}_i \leq \sqrt{\sigma_i^2 + t} \leq \sigma_i + \sqrt{t}$, which implies $\hat{\sigma}^2 \leq (\sigma + J_+ \sqrt{t})^2$. Therefore,

$$\begin{aligned} \mathbb{P}\left(\frac{\hat{\sigma}^2}{J_+^2 \hat{\sigma}_i^2} \geq cM\right) &= \mathbb{P}\left(A_t^c \cup \left\{\frac{\hat{\sigma}^2}{J_+^2 \hat{\sigma}_i^2} \geq cM\right\}\right) + \mathbb{P}\left(A_t \cup \left\{\frac{\hat{\sigma}^2}{J_+^2 \hat{\sigma}_i^2} \geq cM\right\}\right) \\ &\leq \mathbb{P}(A_t^c) + \mathbb{P}\left(A_t, \left\{\frac{\hat{\sigma}^2}{J_+^2 \hat{\sigma}_i^2} \geq cM\right\}\right) \\ &\leq \mathbb{P}(A_t^c) + \mathbb{P}\left(\frac{\hat{\sigma}^2}{J_+^2 \hat{\sigma}_i^2} \geq cM \mid A_t\right) \\ &\leq \mathbb{P}(A_t^c) + \mathbb{P}\left(\frac{(\sigma + \sqrt{t}J_+)^2}{J_+^2(\sigma_i^2 - t)} \geq cM \mid A_t\right). \end{aligned} \quad (25)$$

Notice that $\mathbb{P}\left(\frac{(\sigma + \sqrt{t}J_+)^2}{\sigma_i^2 - t} \geq cM^2 \mid A_t\right)$ is either 0 or 1 since σ_i and σ are constants. We pick t so that this probability is 0. To pick t , notice that,

$$\begin{aligned} \frac{(\sigma + \sqrt{t}J_+)^2}{J_+^2(\sigma_i^2 - t)} &= \frac{\left(\frac{\sigma}{\sigma_i} + \frac{\sqrt{t}J_+}{\sigma_i}\right)^2}{J_+^2\left(1 - \frac{t}{\sigma_i^2}\right)} \\ &\leq \frac{\left(J_+ \sqrt{M} + \frac{J_+ \sqrt{t}M J_+}{\sigma}\right)^2}{J_+^2\left(1 - \frac{t}{\sigma_i^2}\right)} \\ &\leq \frac{M\left(1 + \frac{\sqrt{t}J_+}{\sigma}\right)^2}{1 - \frac{MJ_+^2 t}{\sigma^2}}, \end{aligned} \quad (26)$$

where the last inequality holds as long as $0 < t < \frac{\sigma^2}{MJ_+^2}$ and follows by noting that $\frac{1}{\sigma_i^2} \leq \frac{MJ_+^2}{\sigma^2}$

by assumption. Pick $t = \frac{\sigma^2}{4J_+^2 M}$. Since $0 \leq \sigma \leq 1$, this choice of t implies $\frac{M\left(1 + \frac{\sqrt{t}J_+}{\sigma}\right)^2}{1 - \frac{MJ_+^2 t}{\sigma^2}} \leq 5M$.

Hence, for $c = 5$ and this choice of t , $\mathbb{P}\left(\frac{(\sigma + \sqrt{t}J_+)^2}{J_+^2(\sigma_i^2 - t)} \geq 5M \mid A_t\right) = 0$. Combining Eq. (25) and Eq. (24), we have by a union bound that,

$$\mathbb{P}\left(\frac{\hat{\sigma}^2}{J_+^2 \hat{\sigma}_i^2} \geq 5M\right) \leq 2J_+ \exp\left(-\frac{1}{8}S \frac{\sigma^4}{M^2}\right), \quad (27)$$

for all $i \in [J_+]$. Solving for S by setting the right hand side above to δ yields the claim. \square

We have all the pieces to prove Theorem 3.2. We follow the proof strategy in [6, Theorem 5.2].

Proof. Let $R^* = [z_{+1}^T \circ z_{+1}^T, \dots, z_{+N-1}^T \circ z_{+N-1}^T, z_{+N}^T \circ z_{+N}^T] \in \mathbb{R}^{J_+ \times N^2}$. Notice,

$$\frac{1}{N^2} \|Z_+ Z_+^T - Z(w)Z(w)^T\|_F^2 = (1-w)^T \frac{R^*}{N} \frac{R^{*T}}{N} (1-w). \quad (28)$$

We approximate Eq. (28) with $(1-w)^T \frac{R}{\sqrt{S}} \frac{R^T}{\sqrt{S}} (1-w)$ and bound the error. Suppose

$$D^* := \max_{i,j \in [J_+]} \left| \left(\frac{R^*}{N} \frac{R^{*T}}{N}\right)_{ij} - \left(\frac{R}{\sqrt{S}} \frac{R^T}{\sqrt{S}}\right)_{ij} \right| \leq \frac{\epsilon}{2}.$$

Then,

$$(1-w)^T \frac{R^* R^{*T}}{N} (1-w) - (1-w)^T \frac{R}{\sqrt{S}} \frac{R^T}{\sqrt{S}} (1-w) \leq \sum_{i,j \in [J_+]} |w_i - 1| |w_j - 1| D^* \leq \|w - 1\|_1^2 \frac{\epsilon}{2}. \quad (29)$$

Notice,

$$\begin{aligned} \mathbb{E}_{i_s, j_s} \left[\left(\frac{R}{\sqrt{S}} \frac{R^T}{\sqrt{S}} \right)_{ij} \right] &= \mathbb{E}_{i_s, j_s} \left[\frac{1}{S} \sum_{s=1}^S c_{is} c_{js} \right] \\ &= \frac{1}{S} \sum_{s=1}^S E_{i_s, j_s} [c_{is} c_{js}] \\ &= E_{i_s, j_s} [c_{is} c_{js}] \\ &= \frac{1}{N^2} \sum_{s=1}^{N^2} c_{is} c_{js} \\ &= \left(\frac{R^* R^{*T}}{N} \right)_{ij}. \end{aligned} \quad (30)$$

Hence, the i.i.d. collection of random variables $\{c_{is} c_{js}\}_{s=1}^S$ yields an unbiased estimate of $\left(\frac{R^* R^{*T}}{N} \right)_{ij}$. Each $c_{is} c_{js}$ is bounded by $\frac{1}{J_+^2}$. Therefore, by Hoeffding's inequality and a simple union bound,

$$\mathbb{P} \left(D^* \geq \frac{\epsilon}{2} \right) \leq 2J_+^2 \exp(-2SJ_+^4 \epsilon^2). \quad (31)$$

Setting the right-hand side to $\frac{\delta^*}{2}$ and solving for $\frac{\epsilon}{2}$ implies with probability at least $1 - \frac{\delta^*}{2}$,

$$\frac{\epsilon}{2} \leq \frac{1}{\sqrt{S} J_+^2} \log \left[\frac{4J_+^2}{\delta^*} \right]^{\frac{1}{2}}. \quad (32)$$

Hence, with probability at least $1 - \frac{\delta^*}{2}$,

$$\begin{aligned} \frac{1}{N^2} \|Z_+ Z_+^T - Z(w) Z(w)^T\|_F^2 &\leq (1-w)^T \frac{R}{\sqrt{S}} \frac{R^T}{\sqrt{S}} (1-w) + \|1-w\|_1^2 \frac{1}{\sqrt{S} J_+^2} \log \left[\frac{4J_+^2}{\delta^*} \right]^{\frac{1}{2}} \\ &= \frac{1}{S} \|r - r(w)\|_2^2 + \|1-w\|_1^2 \frac{1}{\sqrt{S} J_+^2} \log \left[\frac{4J_+^2}{\delta^*} \right]^{\frac{1}{2}} \end{aligned}$$

Lemma A.2 implies that there exists a $0 \leq \nu < 1$ such that $\frac{1}{S} \|r - r(w)\|_2^2 \leq \nu^{2J-2}$. Since ν depends on the pairs i_l, j_l picked, we can take ν^* to be the largest ν possible. Since the set of all possible S pairs is finite, that implies $0 \leq \nu^* < 1$. Hence, setting $J = \frac{1}{2} \log_{\nu^*} \left(\frac{\epsilon}{2} \right) + 2$ guarantees that $\frac{1}{S} \|r - r(w)\|_2^2 \leq \frac{\epsilon}{2}$ for any collection of drawn $i_l, j_l, 1 \leq l \leq S$. Assume for any $a \in (0, 1]$ and $\delta > 0$, we can find an M such that

$$\mathbb{P} \left(\max_j \sigma^2 / (J_+^2 \sigma_j^2) > M \right) < a\delta. \quad (33)$$

If Eq. (33) holds, we may assume $\max_j \sigma^2 / (J_+^2 \sigma_j^2) < M$ by setting M large enough since we just need a $1 - \delta$ probabilistic guarantee. By the polytope constraint in Eq. (9), $w_i^* \leq \frac{\hat{\sigma}}{\hat{\sigma}_i}$ for all $i \in [J_+]$. Without loss of generality, assume the first J components of w^* can be the only non-zero values since w^* is at least J sparse. For $S \geq 8 \frac{M^4}{\sigma^4} \log \left(\frac{2J_+}{\delta^2} \right)$, Lemma B.1 implies with probability at least

$1 - \frac{\delta^*}{2}$,

$$\begin{aligned}
\|1 - w^*\|_1^2 &\leq \left(\frac{\hat{\sigma}}{\hat{\sigma}_i} J + (J_+ - J) \right)^2 \\
&\leq (JM J_+ + J_+)^2 \\
&\leq (2JM\sqrt{5}J_+)^2 \\
&\leq 10J_+^2 M^2 J^2 \\
&\leq 10J_+^2 M^2 \frac{(\log \frac{2}{\epsilon})^2}{(\log \nu)^2}
\end{aligned} \tag{34}$$

Therefore, with probability at least $1 - \delta^*$,

$$\frac{1}{N^2} \|Z_+ Z_+^T - Z(w)Z(w)^T\|_F^2 \leq \frac{\epsilon}{2} + \frac{10M^2(\log \frac{2}{\epsilon})^2}{\sqrt{S}(\log \nu)^2} \log \left[\frac{4J_+^2}{\delta^*} \right]^{\frac{1}{2}}. \tag{35}$$

Finally, setting $S \geq \max \left(\frac{100}{\epsilon^2} \left[M \frac{(\log \frac{2}{\epsilon})}{(\log \nu)} \right]^4 \log \left[\frac{4J_+^2}{\delta^*} \right], 8 \frac{M^4}{\sigma^4} \log \left(\frac{2J_+}{\delta^2} \right) \right)$ implies $\frac{1}{N^2} \|Z_+ Z_+^T - Z(w)Z(w)^T\|_F^2 \leq \epsilon$ with probability at least $1 - \delta^*$ which matches the rate provided in Theorem 3.2. It remains to show Eq. (33). Notice that

$$\frac{\sigma}{J_+ \sigma_j} = \frac{1}{J_+} + \frac{1}{J_+} \sum_{i \neq j} \tilde{\sigma}_{ij}, \tag{36}$$

where $\sigma_{ij} := \frac{\sigma_i}{\sigma_j}$. Notice that each σ_{ij} are i.i.d. for $i \neq j$. Let the $\mu_j = \mathbb{E}\sigma_{ij}$ and s_j be the standard deviation of σ_{ij} . Since each σ_j is i.i.d. that implies μ_j and s_j are both constant across j so we drop the subscript. By a union bound, it suffices to show for any $\tau > 0$ we can find an M such that

$$\mathbb{P} \left(\max_{1 \leq j \leq J_+} \frac{1}{J_+} \sum_{i \neq j} \tilde{\sigma}_{ij} > M \right) < \tau. \tag{37}$$

By Chebyshev's inequality,

$$\mathbb{P} \left(\frac{1}{J_+} \sum_{i \neq j} \tilde{\sigma}_{ij} - \mu > \frac{cs}{J_+} \right) \leq \frac{1}{c^2}. \tag{38}$$

Take $c = J_+ \tau$. Then,

$$\mathbb{P} \left(\frac{1}{J_+} \sum_{i \neq j} \tilde{\sigma}_{ij} - \mu > \frac{cs}{J_+} \right) \leq \frac{1}{J_+^2 \tau} < \tau. \tag{39}$$

By a union bound, Eq. (38) implies

$$\mathbb{P} \left(\max_{1 \leq j \leq J_+} \frac{1}{J_+} \sum_{i \neq j} \tilde{\sigma}_{ij} > M \right) < \frac{1}{\tau J_+} < \tau$$

for $M = \mu + s\tau$ as desired.

The proof showing that $\limsup_{J_+ \rightarrow \infty} \nu_{J_+} < 1$ is the same as the proof Theorem 3.4. \square

C Runtime analysis of methods

The ridge regression and PCA runtimes depend on the number of features used, as specified in Table 1, and therefore follow from the first column of the table.

First, we show that using RFM with $J_+ = O\left(\frac{1}{\epsilon} \log \frac{1}{\epsilon}\right)$ number of random features ensures that $\frac{1}{N^2} \|K - \hat{K}\|_F^2 = O(\epsilon)$ with high probability. By a union bound, $\mathbb{P}\left(\frac{1}{N^2} \|K - \hat{K}\|_F^2 \leq \epsilon\right) \geq \mathbb{P}\left(\max_{i,j \in [N]} |K_{ij} - \hat{K}_{ij}| \leq \sqrt{\epsilon}\right)$. Now, Claim 1 of [33] implies

$$\mathbb{P}\left(\max_{i,j \in [N]} |K_{ij} - \hat{K}_{ij}| \geq \sqrt{\epsilon}\right) = O\left(\frac{1}{\epsilon} e^{-J_+ \epsilon}\right). \quad (40)$$

Setting the right-hand side of Eq. (40) to some fixed probability threshold δ^* implies $J_+ = O\left(\frac{1}{\epsilon} \log\left(\frac{1}{\epsilon \delta^*}\right)\right)$. Since δ^* is some fixed constant, $J_+ = O\left(\frac{1}{\epsilon} \log \frac{1}{\epsilon}\right)$ number of random features suffices for an $O(\epsilon)$ error guarantee. Hence, it suffices to use $J_+ = O\left(\frac{1}{\epsilon} \log \frac{1}{\epsilon}\right)$ as the up-projection dimension for both RFM-FW and RFM-JL.

To prove the bounds for RFM-FW, take $S = \Omega(J_+^2 (\log J_+)^2)$. It is straightforward to check that this choice of S satisfies the requirements of Theorem 3.2. By Theorem 3.2, it suffices to set $J = O(\log J_+)$ for an $O(\epsilon)$ error guarantee. Hence, Algorithm 1 takes $O(S J_+ \log J_+)$ time to compute the random feature weights w since Frank-Wolfe has to be run for a total of $O(\log J_+)$ iterations. Finally, it takes $O(N \log J_+)$ to apply these $O(\log J_+)$ weighted random features to the N datapoints. We conclude by proving the time complexity of RFM-JL.

Denote $\tilde{x}_i := (Z_+)_i \in \mathbb{R}^{J_+}$ as the mapped datapoints from RFM. Let $A \in \mathbb{R}^{J \times J_+}$ for $J \leq J_+$ be a matrix filled with i.i.d. $N(0, \frac{1}{J})$ random variables for the JL compression step. Let $f(x) := Ax$. It suffices to pick a J such that,

$$\mathbb{P}\left(\max_{i,j \in [N]} |\tilde{x}_i^T \tilde{x}_j - f(\tilde{x}_i)^T f(\tilde{x}_j)| \geq \sqrt{\epsilon}\right) \leq \delta^* \quad (41)$$

for RFM-JL. We use the following corollary from Kakade and Shakhnarovich [24, Corollary 2.1] to bound the above probability.

Lemma C.1. *Let $u, v \in \mathbb{R}^d$ and such that $\|u\| \leq 1$ and $\|v\| \leq 1$. Let $f(x) = Ax$, where A is a $k \times d, k \leq d$ matrix of i.i.d. $N(0, \frac{1}{k})$ random variables. Then,*

$$\mathbb{P}\left(|u^T v - f(u)^T f(v)| \leq 4e^{-\frac{1}{4}(\epsilon^2 - \epsilon^3)k}\right). \quad (42)$$

$\|\tilde{x}_i\|_2 = 1$ since $\tilde{x}_i = \frac{1}{\sqrt{J_+}} \left(\cos(\omega_1^T x_i + b), \dots, \cos(\omega_{J_+}^T x_i + b)\right)$. Hence, we may apply Lemma C.1 to \tilde{x}_i . By a union bound and an application of Lemma C.1, Eq. (41) is bounded by $O(N^2 e^{-J\epsilon})$. Setting $N^2 e^{-J\epsilon}$ equal to δ^* and solving for J implies that $J = \Omega\left(\frac{1}{\epsilon} \log\left(\frac{N^2}{\delta^*}\right)\right)$. Hence, $J = O\left(\frac{1}{\epsilon} \log N\right)$. Now, $O\left(\frac{1}{\epsilon}\right) = O\left(\frac{J_+}{\log \frac{1}{\epsilon}}\right)$ which implies $J = O\left(\frac{J_+ \log N}{\log \frac{1}{\epsilon}}\right)$. Since $N > J_+ > O\left(\frac{1}{\epsilon}\right)$, $J = \Omega(J_+)$ suffices for an for an $O(\epsilon)$ error guarantee. While the JL algorithm typically takes $O(N J_+ k)$ time to map a $N \times J_+$ matrix to a $N \times k$ matrix, the techniques in Hamid et al. [18, Section 3.5] show that only $O(N J_+ \log J)$ time is required by using the Fast-JL algorithm.

D Impact of kernel approximation

Here we provide the precise error bound and runtimes for kernel ridge regression, kernel SVM, and kernel PCA when using a low-rank factorization ZZ^T of K . We denote $X \subset \mathbb{R}^p$ as the input space and define $c > 0$ such that $K(x, x) \leq c$ and $\hat{K}(x, x) \leq c$ for all $x \in X$. This condition is verified with $c = 1$ for Gaussian kernels for example. All the bounds provided follow from [11, 46], where we simply replace the spectral norm with the Frobenius norm since the Frobenius norm upper bounds the spectral norm.

D.1 Kernel ridge regression

Exact kernel ridge regression takes $O(N^3)$ since K must be inverted. Suppose $K \approx ZZ^T := \hat{K}$, where Z could be found using RFM for example. Running ridge regression with the feature matrix Z just requires computing and inverting the covariance matrix $Z^T Z \in \mathbb{R}^{J \times J}$ which takes $\Theta(\max(J^3, N J^2))$ time. Proposition D.1 quantifies the error between the regressor obtained from K and the one from \hat{K} .

Proposition D.1. (Proposition 1 of [11]) Let \hat{f} denote the regression function returned by kernel ridge regression when using the approximate kernel matrix $\hat{K} \in \mathbb{R}^{N \times M}$, and f^* the function returned when using the exact kernel matrix K . Assume that every response y is bounded in absolute value by M for some $0 < M < \infty$. Let $\lambda := N\lambda_0 > 0$ be the ridge parameter. Then, the following inequality holds for all $x \in X$:

$$\begin{aligned} |\hat{f}(x) - f^*(x)| &\leq \frac{cM}{\lambda_0^2 N} \|\hat{K} - K\|_2 \\ &\leq \frac{cM}{\lambda_0^2 N} \|\hat{K} - K\|_F \\ &= O\left(\frac{1}{N} \|\hat{K} - K\|_F\right) \end{aligned}$$

D.2 Kernel SVM

Kernel SVM regression takes $O(N^3)$ using K since K must be inverted. Again suppose $K \approx ZZ^T := \hat{K}$. Then, training a linear SVM via dual-coordinate decent on Z has time complexity $O(NJ \log \rho)$, where ρ is the optimization tolerance [21].

Proposition D.2. (Proposition 2 of [11]) Let \hat{f} denote the hypothesis returned by SVM when using the approximate kernel matrix \hat{K} , f^* the hypothesis returned when using the exact kernel matrix K , and C_0 be the penalty for SVM. Then, the following inequality holds for all $x \in X$:

$$\begin{aligned} |\hat{f}(x) - f^*(x)| &\leq \sqrt{2}c^{\frac{3}{4}}C_0 \|\hat{K} - K\|_2^{\frac{1}{4}} \left[1 + \frac{\|\hat{K} - K\|_2^{\frac{1}{4}}}{4c}\right] \\ &\leq \sqrt{2}c^{\frac{3}{4}}C_0 \|\hat{K} - K\|_F^{\frac{1}{4}} \left[1 + \frac{\|\hat{K} - K\|_F^{\frac{1}{4}}}{4c}\right]. \\ &= O\left(\|\hat{K} - K\|_F^{\frac{1}{2}}\right). \end{aligned}$$

D.3 Kernel PCA

We follow [46] to understand the effect matrix approximation has on kernel PCA. For a more in-depth analysis, see pg. 92-98 of [46]. Without loss of generality, we assume the data are mean zero.

Let $\Phi(\cdot)$ be the unique feature map such that $k(x, y) = \langle \Phi(x), \Phi(y) \rangle$. Let the feature covariance matrix be denoted as $\Sigma_\Phi := \Phi(X_N)\Phi(X_N)^T$, where $\Phi(X_N) := [\Phi(x_1) \cdots \Phi(x_n)]$. Since the rank of Σ_Φ is at most N , let v_i $1 \leq i \leq N$ be the N singular vectors of Σ_Φ . For certain kernels, e.g., the RBF kernel, the v_i are infinite dimensional. However, the projection of $\Phi(x)$ onto each v_i is tractable to compute via the kernel trick:

$$\Phi(x)^T v_i = \Phi(x) \frac{\Phi(X_N) u_i}{\sqrt{\sigma_i}} = \frac{k_x^T u_i}{\sqrt{\sigma_i}}, \quad (43)$$

where $k_x := (K(x_1, x), \dots, K(x_N, x))$ and u_i is the i th singular vector of K with associated eigenvalue σ_i . Often, the goal is to project $\Phi(x)$ onto the first l eigenvectors of Σ_Φ for dimensionality reduction. To analyze the error of the projection, let P_{V_l} be defined as the subspace V_l spanned by the top l eigenvectors of Σ_Φ . Then, the *average empirical residual* $R_l(K)$ of a kernel matrix K is defined as,

$$\begin{aligned} R_l(K) &:= \frac{1}{N} \sum_{n=1}^N \|\Phi(x_n)\|^2 - \frac{1}{N} \sum_{n=1}^N \|P_{V_l}(\Phi(x_n))\|^2 \\ &= \sum_{i>l} \sigma_i \end{aligned} \quad (44)$$

$R_l(K)$ is simply the spectral error of a low-rank decomposition of Σ_Φ using the SVD. If we instead use \hat{K} for the eigendecomposition, the following proposition bounds the difference between $R_l(K)$ and $R_l(\hat{K})$.

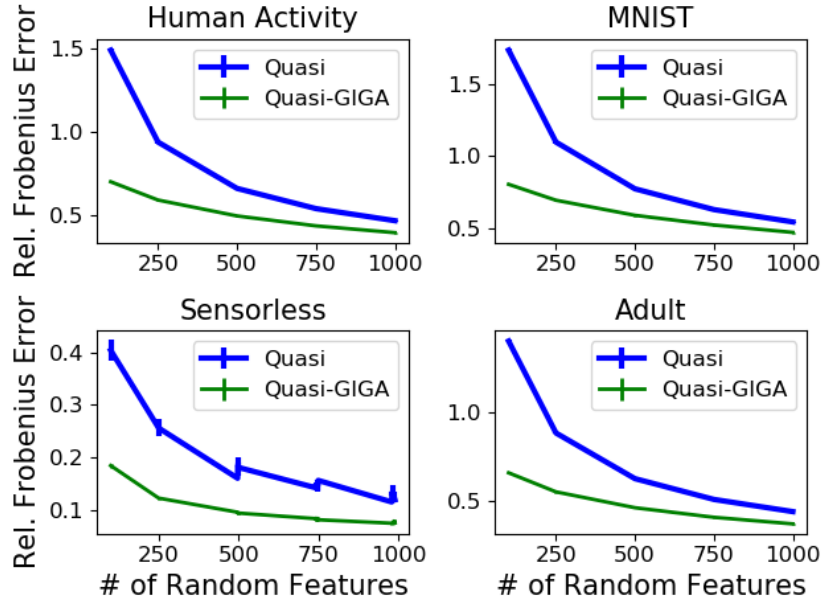


Figure 7: Kernel matrix approximation errors. Lower is better. Each point denotes the average over 20 simulations and the error bars represent one standard deviation. The HALTON sequence was used to generate the quasi random features.

Proposition D.3. (Proposition 5.4 of [46]) For $R_l(K)$ and $R_l(\hat{K})$ defined as above,

$$\begin{aligned}
 |R_l(K) - R_l(\hat{K})| &\leq \left(1 - \frac{l}{N}\right) \|K - \hat{K}\|_2 \\
 &\leq \left(1 - \frac{l}{N}\right) \|K - \hat{K}\|_F.
 \end{aligned}$$

E Additional Experiments

As stated in Section 4, our method may be applied on top of other random feature methods. In particular, many previous works have reduced the number of random features needed for a given level of approximation by sampling them from a different distribution (e.g., through importance sampling or Quasi-Monte-Carlo techniques). Regardless of the way the random features are sampled, our method can still be used for compression.

To demonstrate this point further, we consider generating random features using Quasi-Monte-Carlo [1]. Quasi random features work by generating a sequence of points from a (low-discrepancy) grid of points in $[0, 1]^p$. Points are sampled from the target random-features distribution Q by applying the inverse CDF of Q on each of these points in the sequence. In Avron et al. [1], the authors showed that generating random features in this way improved performance over the classical random features method provided in Rahimi and Recht [33]. In Fig. 7 and Fig. 8, we see that our method is able to compress the number of quasi random features, which is similar to the behavior in Fig. 1 and Fig. 2. Note that the experimental setup is exactly the same as in Section 4 except that the random features are now generated using Quasi-Monte-Carlo.

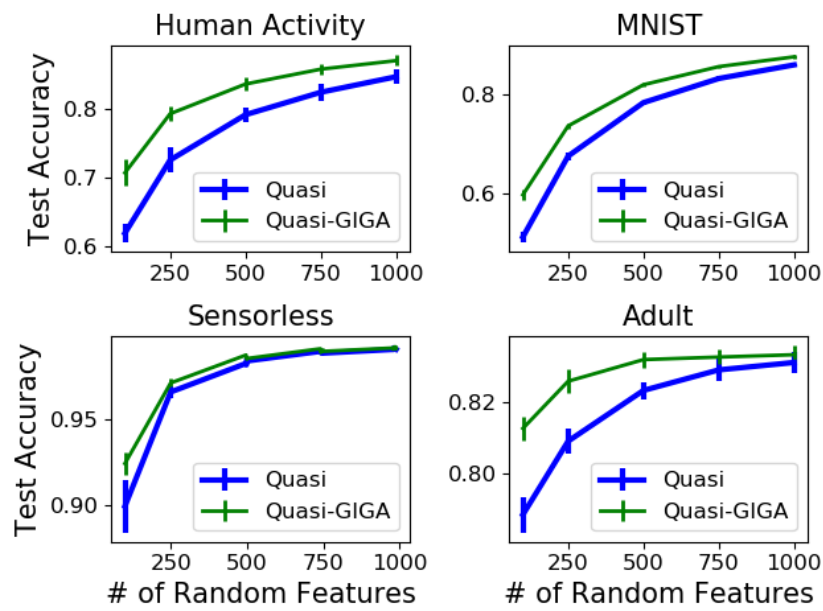


Figure 8: Classification accuracy. Higher is better. Each point denotes the average over 20 simulations and the error bars represent one standard deviation. The HALTON sequence was used to generate the Quasi random features.

References

- [1] H. Avron, V. Sindhvani, J. Yang, and M. W. Mahoney. Quasi-Monte Carlo feature maps for shift-invariant kernels. *Journal of Machine Learning Research*, pages 1–38, 2016.
- [2] H. Avron, M. Kapralov, C. Musco, C. Musco, A. Velingker, and A. Zandieh. Random Fourier features for kernel ridge regression: Approximation bounds and statistical guarantees. In *International Conference on Machine Learning*, 2017.
- [3] M. Balcan, A. Blum, and S. Vempala. On kernels, margins, and low-dimensional mappings. In *Algorithmic Learning Theory*, pages 1–12, 2008.
- [4] B. Boser, I. Guyon, and V. Vapnik. A training algorithm for optimal margin classifiers. In *Workshop on Computational Learning Theory*, pages 144–152, 1992.
- [5] T. Campbell and T. Broderick. Bayesian coresets construction via greedy iterative geodesic ascent. In *International Conference on Machine Learning*, 2018.
- [6] T. Campbell and T. Broderick. Automated scalable Bayesian inference via Hilbert coresets. *Journal of Machine Learning Research*, 2019.
- [7] E. Candes and T. Tao. The Dantzig selector: Statistical estimation when p is much larger than n . *The Annals of Statistics*, pages 2313–2351, 2007.
- [8] W. Chang, C. Li, Y. Yang, and B. Poczos. Data-driven random Fourier features using Stein effect. In *International Joint Conference on Artificial Intelligence*, pages 1497–1503, 2017.
- [9] S. Chen, D. Donoho, and M. Saunders. Atomic decomposition by basis pursuit. *SIAM Journal on Scientific Computing*, pages 33–61, 1998.
- [10] K. Chwialkowski, H. Strathmann, and A. Gretton. A kernel test of goodness of fit. In *International Conference on Machine Learning*, 2016.
- [11] C. Cortes, M. Mohri, and A. Talwalkar. On the impact of kernel approximation on learning accuracy. In *International Conference on Artificial Intelligence and Statistics*, 2010.
- [12] A. Daniely, R. Frostig, V. Gupta, and Y. Singer. Random features for compositional kernels. *arXiv:1703.07872*, 2017.
- [13] P. Drineas and M. Mahoney. On the Nyström method for approximating a gram matrix for improved kernel-based learning. *Journal of Machine Learning Research*, pages 2153–2175, 2005.
- [14] A. El Alaoui and M. Mahoney. Fast randomized kernel methods with statistical guarantees. In *Advances in Neural Information Processing Systems*, 2015.
- [15] A. Gretton, K. Fukumizu, C. H., L. Song, B. Schölkopf, and A. Smola. A kernel statistical test of independence. In *Advances in Neural Information Processing Systems*, pages 585–592, 2008.
- [16] A. Gretton, K. Borgwardt, M. Rasch, B. Schölkopf, and A. Smola. A kernel two-sample test. *Journal of Machine Learning Research*, pages 723–773, 2012.
- [17] N. Halko, P. Martinsson, and J. Tropp. Finding structure with randomness: Probabilistic algorithms for constructing approximate matrix decompositions. *SIAM Review*, pages 217–288, 2011.
- [18] R. Hamid, Y. Xiao, A. Gittens, and D. DeCoste. Compact random feature maps. In *International Conference on International Conference on Machine Learning*, 2014.
- [19] T. Hofmann, B. Schölkopf, and A. Smola. Kernel methods in machine learning. *The Annals of Statistics*, pages 1171–1220, 2008.
- [20] J. Honorio and Y.-J. Li. The error probability of random Fourier features is dimensionality independent. *arXiv:1710.09953*, 2017.

- [21] C. Hsieh, K. Chang, C. Lin, S. Keerthi, and S. Sundararajan. A dual coordinate descent method for large-scale linear SVM. In *International Conference on Machine Learning*, pages 408–415, 2008.
- [22] P. Huang, H. Avron, T. Sainath, V. Sindhwani, and B. Ramabhadran. Kernel methods match deep neural networks on TIMIT. In *International Conference on Acoustics, Speech and Signal Processing*, pages 205–209, May 2014.
- [23] W. Johnson, J. Lindenstrauss, and G. Schechtman. Extensions of Lipschitz maps into Banach spaces. *Israel Journal of Mathematics*, pages 129–138, 1986.
- [24] S. Kakade and G. Shakhnarovich. Lecture notes in large scale learning, 2009. URL <http://ttic.uchicago.edu/~gregory/courses/LargeScaleLearning/lectures/jl.pdf>.
- [25] P. Kar and H. Karnick. Random feature maps for dot product kernels. In *International Conference on Artificial Intelligence and Statistics*, pages 583–591, 2012.
- [26] Q. Le, T. Sarlos, and A. Smola. Fastfood - approximating kernel expansions in loglinear time. In *International Conference on Machine Learning*, 2013.
- [27] P. Li, T. Hastie, and K. Church. Very sparse random projections. In *International Conference on Knowledge Discovery and Data Mining*, pages 287–296, 2006.
- [28] W. Lim, R. Du, B. Dai, K. Jung, L. Song, and H. Park. Multi-scale Nystrom method. In *International Conference on Artificial Intelligence and Statistics*, 2018.
- [29] F. Marguerite and W. Philip. An algorithm for quadratic programming. *Naval Research Logistics Quarterly*, pages 95–110, 1956.
- [30] S. Mendelson. On the performance of kernel classes. *Journal of Machine Learning Research*, pages 759–771, 2003.
- [31] C. Musco and C. Musco. Recursive sampling for the Nyström method. In *Advances in Neural Information Processing Systems*, 2017.
- [32] J. Pennington, F. Yu, and S. Kumar. Spherical random features for polynomial kernels. In *Advances in Neural Information Processing Systems*, pages 1846–1854, 2015.
- [33] A. Rahimi and B. Recht. Random features for large-scale kernel machines. In *Neural Information Processing Systems*, 2007.
- [34] A. Rahimi and B. Recht. Random features for large-scale kernel machines. In *Advances in Neural Information Processing Systems*, pages 1177–1184, 2008.
- [35] A. Rudi and L. Rosasco. Generalization properties of learning with random features. In *Advances in Neural Information Processing Systems*, 2017.
- [36] A. Rudi, R. Camoriano, and L. Rosasco. Less is more: Nyström computational regularization. In *Advances in Neural Information Processing Systems*, 2015.
- [37] W. Rudin. *Fourier Analysis on Groups*, chapter The Basic Theorems of Fourier Analysis. Wiley, 1994.
- [38] Y. Samo and S. Roberts. Generalized spectral kernels. *arXiv:1506.02236*, 2015.
- [39] C. Saunders, A. Gammerman, and V. Vovk. Ridge regression learning algorithm in dual variables. In *International Conference on Machine Learning*, pages 515–521, 1998.
- [40] B. Schölkopf and A. Smola. *Learning with Kernels: Support Vector Machines, Regularization, Optimization, and Beyond*. MIT Press, 2001.
- [41] B. Schölkopf, A. Smola, and K. Müller. Kernel principal component analysis. In *Artificial Neural Networks*, pages 583–588, 1997.
- [42] W. Shen, Z. Yang, and J. Wang. Random features for shift-invariant kernels with moment matching. In *Association for the Advancement of Artificial Intelligence Conference*, 2017.

- [43] B. Sriperumbudur and N. Sturge. Approximate kernel PCA using random features: Computational vs. statistical trade-off. *arXiv:1706.06296*, 2017.
- [44] B. Sriperumbudur, A. Gretton, K. Fukumizu, B. Schölkopf, and G. Lanckriet. Hilbert space embeddings and metrics on probability measures. *Journal of Machine Learning Research*, pages 1517–1561, 2010.
- [45] D. Sutherland and J. Schneider. On the error of random Fourier features. In *Conference on Uncertainty in Artificial Intelligence*, pages 862–871, 2015.
- [46] A. Talwalkar. *Matrix Approximation for Large-scale Learning*. PhD thesis, New York University, 2010.
- [47] R. Tibshirani. Regression shrinkage and selection via the lasso. *Journal of the Royal Statistical Society, Series B*, pages 267–288, 1994.
- [48] V. Vapnik. *Statistical Learning Theory*. John Wiley & Sons, New York, 1998.
- [49] V. Vapnik, S. Golowich, and A. Smola. Support vector method for function approximation, regression estimation and signal processing. In *Advances in Neural Information Processing Systems*, pages 281–287, 1997.
- [50] C. Williams and M. Seeger. Using the Nyström method to speed up kernel machines. In *Advances in Neural Information Processing Systems*, pages 682–688, 2001.
- [51] T. Yang, Y. Li, M. Mahdavi, R. Jin, and Z. Zhou. Nyström method vs random Fourier features - a theoretical and empirical comparison. In *Advances in Neural Information Processing Systems*, 2012.
- [52] Y. Yang, M. Pilanci, and M. J. Wainwright. Randomized sketches for kernels: Fast and optimal nonparametric regression. *The Annals of Statistics*, pages 991–1023, 2017.
- [53] F. Yu, A. Suresh, K. Choromanski, D. Holtmann-Rice, and S. Kumar. Orthogonal random features. In *Advances in Neural Information Processing Systems*, pages 1975–1983, 2016.
- [54] K. Zhang, J. Peters, D. Janzing, and B. Schölkopf. Kernel-based conditional independence test and application in causal discovery. In *Conference on Uncertainty in Artificial Intelligence*, pages 804–813, 2011.